Available online at www.sciencedirect.com
ScienceDirect
Catalysis Today 120 (2007) 351–357
CATALYSIS TODAY
www.elsevier.com/locate/cattod

Hydrogen diffusion in quasicrystalline and amorphous Zr–Cu–Ni–Al

J. Dolinšek [a,*], T. Apih [a], M. Klanjšek [a], Hae Jin Kim [b], U. Köster [c]

[a] J. Stefan Institute, University of Ljubljana, Jamova 39, SI-1000 Ljubljana, Slovenia
[b] Energy Nano Material Team, Frontier Research Laboratory, Korea Basic Science Institute (KBSI), 52 Yeoeun, Yuseong, Daejon 305-333, Republic of Korea
[c] Department of Biochemical and Chemical Engineering, University of Dortmund, D-44221 Dortmund, Germany

Available online 25 October 2006

Abstract

We report on the direct determination of the hydrogen self-diffusion constant D in the hydrogen-storage $Zr_{69.5}Cu_{12}Ni_{11}Al_{7.5}$ alloy, prepared in both the icosahedral quasicrystalline and the bulk metallic glass phases, using the technique of NMR diffusion in a static fringe field of a superconducting magnet. The diffusion constant exhibits strong dependence on temperature and hydrogen concentration. D was found to obey classical Arrhenius thermally activated over-barrier hopping form, whereas the significant decrease of D with increasing hydrogen-to-metal concentration ratio H/M is a result of two effects – the increase of the activation energy for hydrogen jumps between interstitial sites due to lattice expansion upon hydrogenation and the decreasing number of available empty interstitials due to site blocking and creation of defects in the lattice during hydrogen loading. The actual alloy structure – the icosahedral, approximant or metallic glass – appears to be less important for the hydrogen diffusivity.

Keywords: Quasicrystals; Metallic glasses; Hydrogen diffusion in solids; Nuclear magnetic resonance

1. Introduction

Key properties of good hydrogen storage materials are: (i) high hydrogen storage capacity, (ii) ability to load and unload hydrogen at reasonable values of pressure and temperature and within a reasonable time and (iii) ability to repeat this cycle many times without degradation of the storage material. Examples of technologically widespread hydrogen storage metal hydrides [1] are $LaNi_5$, used in hydride batteries, which can absorb hydrogen up to hydrogen-to-metal (H/M) ratio 1.1 or to capacity per weight 1.5%, and TiFe with $H/M = 0.9$ and 1.6 wt.%. While the loading capacity is better for Mg ($H/M = 2.0$ and 7.7 wt.%) and V ($H/M = 2.0$ and 3.8 wt.%), Mg is flammable and requires higher unloading temperature than is typical for the exhaust gas from an internal combustion engine, and the materials costs for V are too high for its widespread use. It has been recently demonstrated [1] that Ti- and Zr-based quasicrystals (QCs)—long-range ordered nonperiodic alloys whose structures exhibit crystallographically forbidden symmetries like fivefold rotation axis—exhibit favorable hydrogen storage properties. Examples are icosahedral (*i*) Ti–Zr/Hf–Ni [2–6] and Zr–Cu–Ni–Al [7–13], which can be prepared in either the QC or the bulk metallic glass (BMG) state. The total loading capacity of *i*-QCs is competitive to the best known H-storage crystalline alloys ($H/M \approx 2.0$ can be reached, whereas maximum capacity per weight 2.5% is less favorable), the absorption and desorption of hydrogen is quick and the alloys are made of low-cost materials. Based on initial desorption data for icosahedral $Ti_{45}Zr_{38}Ni_7$, binding enthalpy for the least tightly bound hydrogen is small, of the order −0.10 eV/atom [1].

Hydrogen in a metal is in an ionized state (for discussion see [14]), a proton surrounded by an excess of conduction electrons that screen its positive charge at a distance on the order of 1 nm. There is no one electron bound to the proton. The protons occupy interstitial sites, the holes in the lattice between the atoms of the metal host. The most favorable sites, those occupied by the first hydrogen atoms absorbed, are in most cases the tetrahedral interstitials like the positions (1/4, 1/4, 1/4) in the fcc cubic cell. Some materials continue to absorb hydrogen after all the tetrahedral interstitials are filled, by capturing protons in octahedral interstitials, like the position (1/2, 0, 0) in the fcc cubic cell. Usually not all interstitials can be occupied simultaneously; according to the Switendick criterion

* Corresponding author. Tel.: +386 1 4773 740; fax: +386 1 4773 191.
E-mail address: jani.dolinsek@ijs.si (J. Dolinšek).

0920-5861/$ – see front matter © 2006 Elsevier B.V. All rights reserved.
doi:10.1016/j.cattod.2006.09.008

[15], no two hydrogen atoms can be closer than 0.21 nm. High hydrogen storage capacity of *i*-QCs originates from specific local structure of these aperiodic compounds [1]. The basic building block of *i*-QCs is usually a multi-shell atomic cluster of icosahedral symmetry, which aperiodically repeats over the structure. The polytetrahedral local atomic order within these clusters is at the origin of a high number of tetrahedral and octahedral interstitials. For example, the Mackay icosahedral cluster, the building block of the Al–Pd–Mn-type *i*-QCs and the related crystalline phases in Al–Mn, Ti–Cr–Si–O, and Ti–Zr–Fe alloys, contains 20 tetrahedral interstitials inside its inner icosahedral shell and 60 tetrahedral interstitials and 20 octahedral interstitials between its inner and outer shells. The Bergman atomic cluster, the building block of the Al–Mg–Zn-type *i*-QCs and the related crystalline phases in Al–Li–Cu and Ti–Zr–Ni alloys, contains 20 tetrahedral interstitials within its inner shell, 120 between the inner and the outer shells, and no octahedral interstitials. Therefore, the high hydrogen storage capacity due to specific polytetrahedral local atomic order and favorable hydrogen chemistry (low binding energy to metal atoms), together with the low-cost materials, make the Ti- and Zr-based *i*-QCs promissing materials for the hydrogen storage application.

2. NMR determination of hydrogen diffusion in metal hydrides

Proper hydrogen-storage materials show the ability to get hydrogen into and out of the metal easily and within a reasonable time. This is related to the mobility of hydrogen atoms within the crystalline lattice, so that knowledge of the hydrogen self-diffusion coefficient in a metal host is of high importance. There exist many methods to determine the hydrogen diffusion constant in metal hydrides [16–18], among which the nuclear magnetic resonance (NMR) has probably been applied to more hydrides than any other technique. Various NMR techniques, including spin–lattice relaxation in the laboratory-, rotating- and dipolar frames, NMR line width and diffusion in a magnetic field gradient are suitable to characterize diffusion coefficients in the range between 10^{-12} and 10^{-4} cm^2/s. Out of these techniques, only the diffusion in a field gradient gives a direct, model-independent value of the diffusion constant D, whereas all other techniques yield an indirect information, the correlation time τ_c of the fluctuating local magnetic fields. Assuming that τ_c fluctuations arise predominantly from the translational diffusion of protons (which is in many cases a crude and not well justified assumption), the diffusion coefficient may be estimated from the relation $D = f_T a^2/6\tau_c$. Here a is the mean jump distance and f_T is the structure-sensitive ''tracer correlation function'', ranging usually between 0.5 and 1. Except for some simple structures, a and f_T are not easily obtained. Regarding the NMR diffusion technique in a magnetic field gradient, the most commonly employed method is that of Stejskal and Tanner [19], which uses pulsed field gradient (PFG). The technically available PFG values limit the sensitivity of this technique to the range $D \geq 10^{-8}$ cm^2/s. The PFG method was successfully applied to simple-structure metal hydrides, like the elemental fcc PdH_x and TiH_x [18] and the $Pd_{1-x}Ag_xH_y$ alloys [20], where D was determined at temperatures where its value was in the range 10^{-6} to 10^{-8} cm^2/s. The more complicated structure and/or structural and chemical disorders make the hydrogen diffusion in QCs slower with $D < 10^{-8}$ cm^2/s, which is below the sensitivity threshold of the PFG method. There exists, however, another NMR method for the diffusion constant determination with extended sensitivity towards much lower D values. This is the method of NMR diffusion in a static fringe field (SFF) of a superconducting magnet, introduced in 1991 by Kimmich et al. [21]. The SFF method takes advantage of the ultrahigh magnetic field gradients (typically up to 80 T/m) of the highly stable static fringe field of an NMR superconducting magnet, extending sensitivity to molecular diffusion down to $D \geq 10^{-11}$ cm^2/s. SFF diffusion measurements were successfully applied in the past to systems such as supercooled liquids, molecular crystals, long-chain polymers and systems of confined mesoscopic geometries and fractal structures [22], whereas measurements of hydrogen diffusion in metal hydrides by this technique were reported only recently [12,13]. For the hydrogen storage QCs, the SFF method offers a promising way to determine directly the hydrogen diffusion coefficient. There, the D values are below the detection threshold of the PFG method at practically all temperatures of interest, because at elevated temperatures (e.g. above 350 °C for Ti–Zr–Ni [2]) the Ti- and Zr-based hydrogen-storage *i*-QCs structurally decompose and transform into more stable crystalline hydride phases.

In our diffusion studies, to be presented in the following, the SFF experiments were conducted in a superconducting magnet with the center field 6.3 T (corresponding to the ^{1}H resonance frequency of 270 MHz). The experimental setup, including the fringe field data of this magnet, was published before [23]. The probe head was fine-positioned at one edge of the superconducting coil, where the proton resonance frequency amounted $\nu(^1\mathrm{H}) = 100.0$ MHz and the gradient was $g = 49$ T/m. The stimulated spin echo pulse sequence ($\pi/2 - \tau - \pi/2 - t - \pi/2 - \tau -$ echo) was used with the $\pi/2$ rf pulse length of 1 μs. In the presence of diffusing nuclei in a constant field gradient g, the amplitude of the spin echo decays with time according to [21]:

$$A = A_0 \exp(-2\tau/T_2) \exp(-t/T_1) \exp\left(-\gamma^2 g^2 D \tau^2 \left(t + \frac{2}{3}\tau \right) \right) \quad (1)$$

Here A_0 is the initial echo amplitude, T_1 and T_2 are the spin–lattice and spin–spin relaxation times, respectively, γ is the nuclear gyromagnetic ratio and D is the diffusion constant. In order to extract D, one first varies systematically the ''diffusion time'' t, keeping the time τ fixed. The echo amplitude than decays in t with the constant $R_1 = 1/T_1 + \gamma^2 g^2 D \tau^2$. The experiment is repeated for a set of τ values and the resulting R_1 is plotted as a function of τ^2. Typical R_1 versus τ^2 curves at different temperatures are shown as an inset in Fig. 1. The slope of the straight line yields the diffusion constant D, whereas the

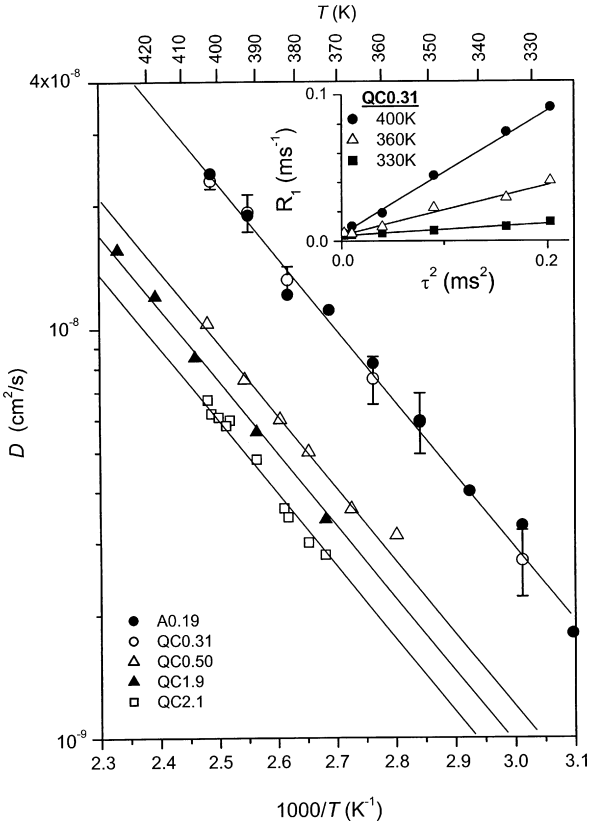

Fig. 1. Temperature-dependent hydrogen diffusion constant D in the ZrCuNiAl icosahedral alloy hydrogenated to different H/M (samples described in the text). Solid lines are fits with $D = D_0 \exp(-E_a/k_BT)$, using in all cases the same value of the activation energy $E_a = 365$ meV. Typical R_1 vs. τ^2 curves, from which D is extracted, are shown as an inset.

zero-intercept is $1/T_1$, which is independently known from the relaxation-time measurements.

3. Hydrogen diffusion in partially quasicrystalline $Zr_{69.5}Cu_{12}Ni_{11}Al_{7.5}$

Our hydrogen diffusion measurements by the SFF method were performed in a quaternary icosahedral alloy $Zr_{69.5}Cu_{12}Ni_{11}Al_{7.5}$ [12] (in the following abbreviated as ZrCuNiAl). This alloy exhibits exceptional glass forming ability, and is one of the few known systems [7] that undergo transformation from the glassy to the icosahedral quasicrystalline state by annealing the amorphous as-cast material (melt-spun ribbons) above the glass transition temperature 372 °C. The details of the material preparation, hydrogen loading and desorption, stability, structural quality and structure transformation upon hydrogenation are published elsewhere [7–11]. During annealing, a microstructure of icosahedral QCs develops within the sea of amorphous material, the largest attainable quasicrystalline volume being $V_{QC} \approx 90\%$. Since the storage capacity was found higher and the hydrogen absorption kinetics faster [11] for samples with a quasicrystalline volume of about 50% than for the fully quasicrystalline ones (90%), our experiments were conducted on $V_{QC} \approx 50\%$ samples. The hydrogen diffusion results presented in the following should thus not be considered as specific to the QC phase, but to quasicrystalline microcrystals embedded in an amorphous matrix. The samples were hydrogen-loaded electrolitically in a 2:1 glycerine-phosphoric acid at 25 °C and a current density of $j = 10$ A/m^2. The hydrogen content was determined by weighting with a Mettler microbalance with accuracy of ± 1 μg and from the shift of the X-ray lines [8] towards smaller angles due to lattice expansion. The increase of the quasilattice constant by about 10% at $H/M = 2.0$ in the ZrCuNiAl compares well to the 7% increase observed in the Ti-based QCs with $H/M = 1.6$ [2]. Our study included five samples loaded to different H/Ms: (i) an amorphous as-cast material loaded to $H/M = 0.192$ (hereafter referred to as the sample A0.19), and four quasicrystalline samples loaded to (ii) $H/M = 0.309$ (QC0.31 sample), (iii) $H/M = 0.50$ (QC0.50), (iv) $H/M = 1.9$ (QC1.9) and (v) $H/M = 2.1$ (QC2.1). Since the amount of hydrogen outgassing soon after the hydrogenation has not been studied, the high H/M values of 1.9 and 2.1 should not be taken literally. An increased degree of hydrogenation leads to an increased nearest neighbour distance of both, the QC phase and the amorphous matrix, accompanied by a phase transformation of the QC from icosahedral to approximant phases [11] and its final amorphization at H/M values above 1.0. X-ray diffraction and transmission electron microscopy (TEM) investigations [8] showed that, after hydrogen degassing, the quasilattice parameter is restored totally to its initial ($H/M = 0$) value, whereas the remaining weakened contrast of the bright-field TEM images and the absence of weak diffraction lines indicate the presence of a high density of defects, not present in the virgin material. These defects are created during hydrogen loading and are not annealed-out after complete hydrogen desorption.

The diffusion constants were determined in the interval between room temperature and 440 K and the data are displayed in Fig. 1. Within this temperature interval, the D values of all samples are in the range between 1.8×10^{-9} and 2×10^{-8} cm^2/s. The $D(T)$ data points fall on straight lines in the log D versus $1/T$ plot, indicating a simple classical (Arrhenius) over-barrier-hopping hydrogen diffusion with $D = D_0 \exp(-E_a/k_BT)$, where E_a is the activation energy. Within our experimental precision (~10%), the $D(T)$ curves of all samples appear to run in parallel, so that the variation of the activation energy between the samples is within the experimental error. The variation of E_a in samples loaded to different H/M is, however, expected on the basis of lattice expansion data upon hydrogenation, as increased interatomic distances should be accompanied by increased potential barriers for the proton jumps between different interstitial sites. The $D(T)$ fits (solid lines in Fig. 1) are all made with the same value of the activation energy $E_a = 365 \pm 15$ meV, which should be considered as the average E_a of all samples. Here it is important to stress that this E_a value is model-independent and hence does not suffer from the model-dependent analysis as in the case when extracted from the τ_c data of the NMR relaxation experiments. The translational shifts of the $D(T)$ curves show that the prefactors $D_0 \approx a^2/6\tau_\infty$ (where τ_∞^{-1} is the hydrogen jump attempt frequency defined by the Arrhenius relation $\tau_c = \tau_\infty \exp(E_a/k_BT)$) are different. Samples loaded to higher H/M values show systematically lower D_0 values (Fig. 2). A trivial explanation for this decrease could be the "site-blocking" effect,

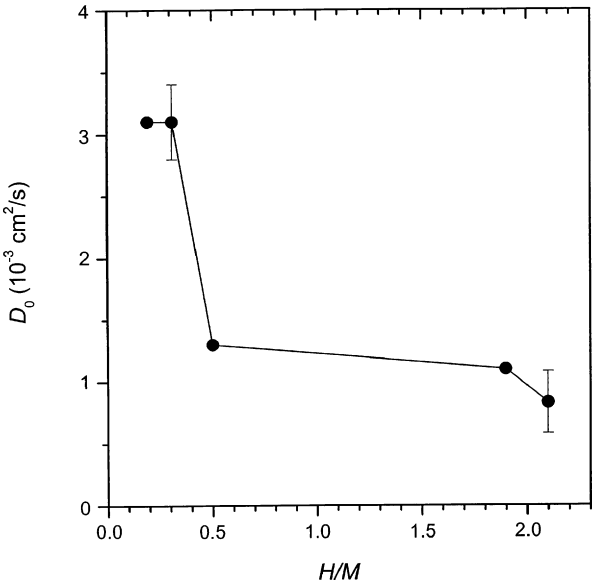

Fig. 2. The H/M-dependence of the diffusion prefactor D_0 (solid circles).

where the increased occupancy of interstitial sites for increasing $H/M = x$ would result in a decrease of the attempt jump frequency as $(2 - x)\tau_\infty^{-1}$ [18] (where 2 is taken as the maximum possible x for the ZrCuNiAl), so that the diffusion coefficient scales with x as $D = (2 - x)D_0 \exp(-E_a/k_BT)$. This should lead to a linear decrease of the prefactor $(2 - x)D_0$ with increasing H/M, in contrast to a much faster variation of the experimental D_0 values displayed in Fig. 2. According to this, the H/M dependence of D_0 may not be explained only by the site-blocking effect. It can also not be attributed to the gradual amorphization of the QC samples upon the hydrogenation-induced phase transformation to the amorphous state, as the amorphous sample A 0.19 shows in fact the highest diffusivity, equal to that of the QC0.31 sample. The decrease of D with H/M should thus also be affected by the increase of the activation energy (though not observed unambiguously in our experiment). In addition, the above discussed TEM- and X-ray detected defects in the lattice, introduced by the hydrogen loading, can also contribute significantly to the H/M-dependent decrease of D. These defects locally distort the tetrahedral coordination of the interstitial sites, making the number of available hydrogen sites smaller with increasing H/M. The concentration of defects strongly depends on H/M, but is rather independent of the actual crystalline structure (as tetrahedral sites are present in all phases—the QC, the approximant and the amorphous). Finally, it is worth noting that the hydrogen diffusivity in the investigated samples is fairly independent of the actual crystalline structure (D values of the starting amorphous material A0.19 and the quasicrystalline QC0.31 sample, both loaded to small H/M, are practically equal).

4. Hydrogen diffusion in bulk metallic glass $Zr_{69.5}Cu_{12}Ni_{11}Al_{7.5}$

Although the above-presented SFF NMR study of hydrogen diffusion in the *i*-QC $Zr_{69.5}Cu_{12}Ni_{11}Al_{7.5}$ was successful in determining the temperature dependence of D, it was inconclusive regarding specific features of the hydrogen motion in this alloy from several aspects. The investigated material was not fully quasicrystalline, but the QC volume was about 50%, forming QC micrograins within an amorphous matrix. Upon hydrogenation, QC micrograins undergo a continuous-like phase transformation from icosahedral to approximant phases of increasingly higher order [11,24] and finally become amorphous at H/M values above 1.0. The structure is therefore changing all the time with increasing H/M. The study also included only a small number (four) of initially ($H/M = 0$) icosahedral samples hydrogenated to unevenly spaced H/M values (0.3, 0.5, 1.9 and 2.1), so that the H/M dependence of D could be discussed only qualitatively. The change of the hydrogen hopping activation energy E_a with H/M could also not be claimed unambiguously; if existing, it was within the experimental error of about 10%. In order to elaborate further these issues, we performed a new set of SFF diffusion experiments on the same $Zr_{69.5}Cu_{12}Ni_{11}Al_{7.5}$ material, this time in the amorphous (bulk metallic glass) state, in order to avoid the phase transformation problem upon hydrogenation. BMGs are believed to show structural similarity to *i*-QCs in the range of short-range order (SRO). On the atomic level, polytetrahedral packing is obvious in both cases, which in three-dimensional space necessarily means a non-periodic arrangement of non-regular tetrahedra. Starting from an arbitrary "central" atom, the first nearest-neighbour shell preferably forms an icosahedron, around which the number of possible atomic configurations increases rapidly towards higher coordination shells. This viewpoint led to various types of icosahedral cluster models, which exists both for *i*-QCs [25] and BMGs [26], thus promoting the idea of an icosahedral SRO in metallic glasses.

In the following we present the temperature- and H/M-dependent hydrogen self-diffusion coefficient D in the BMG phase of ZrCuNiAl. For better sampling of the H/M-dependent properties, the experiment included twelve samples hydrogenated to approximately evenly spaced H/Ms: 0.05, 0.1, 0.17, 0.21, 0.5, 0.74, 0.85, 0.9, 1.1, 1.2, 1.6 and 1.9.

The diffusion constant in the ZrCuNiAl BMG phase [13] was determined in the interval between room temperature and 420 K and the data are displayed in Fig. 3. Within this temperature range, the D values of all samples are in the range between 1×10^{-9} and 3×10^{-8} cm^2/s, which is the same range as found in the partially icosahedral state of the same material. The $D(T)$ data points again fall on straight lines in the log D versus $1/T$ plot, indicating classical over-barrier-hopping hydrogen diffusion. A fit of the $D(T)$ data with the Arrhenius thermally activated form yielded a H/M-dependent activation energy (Fig. 4a). In the low hydrogen-concentration range, $H/M < 0.2$, E_a can be considered roughly as constant within the experimental precision, its value (taken as the average over the samples hydrogenated to low H/M values 0.05, 0.1, 0.17 and 0.21) amounts to $E_a = 402 \pm 4$ meV. A closer inspection of the E_a data points in this low H/M regime indicates even a tendency of a slight *decrease* of the activation energy with increasing H/M, but the effect cannot be claimed unambiguously as it is

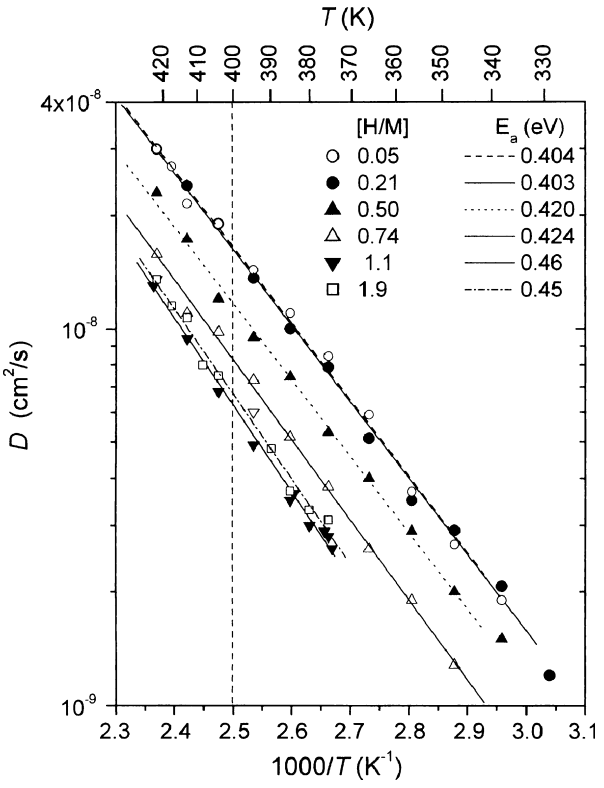

Fig. 3. Temperature-dependent hydrogen diffusion constant D of the ZrCuNiAl bulk metallic glass. The data of a representative set of six samples (out of 12 investigated) hydrated to different H/M values are displayed. Lines are fits with $D = D_0 \exp(-E_a/k_B T)$. The respective H/M and E_a values are indicated on the graph. Dashed vertical line indicates the temperature 400 K at which the D values in Fig. 4b were extracted from the fits.

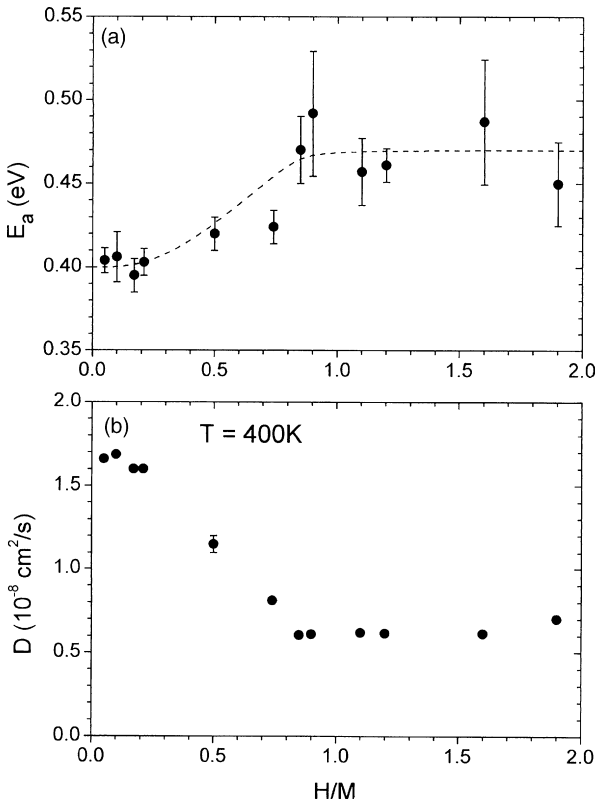

Fig. 4. H/M-dependent (a) activation energy E_a for hydrogen diffusion in the ZrCuNiAl bulk metallic glass (dashed line is a guide for the eye) and (b) hydrogen diffusion constant D at $T = 400$ K extracted from the fits in Fig. 3.

comparable to the experimental error. In the intermediate range, $0.2 < H/M < 0.9$, E_a increases monotonously, whereas at high concentrations, $H/M > 0.9$, it saturates to a plateau $E_a \approx 470$ meV, the total increase in the whole investigated H/M range being 17% of the $H/M \to 0$ value. A similar H/M dependence is observed also in the diffusion coefficient D, which is plotted in Fig. 4b as a function of H/M at a fixed temperature 400 K (the values are taken from the fits in Fig. 3). In the low concentration regime, $H/M < 0.2$, D is again approximately H/M-independent or, more likely, it exhibits an insignificant maximum at $H/M = 0.1$. At intermediate concentrations, $0.2 < H/M < 0.9$, D decreases in a linear-like manner and finally reaches a constant plateau for $H/M > 0.9$. The total decrease of D from $H/M = 0.2$ to 0.9 is by a factor $D_{0.2}/D_{0.9} = 2.7$.

The anomalous H/M-dependence of E_a and D from Fig. 4 at low hydrogen concentration ($H/M < 0.2$) can be explained within the following picture. Based on the model of Kirchheim [27], very small amounts of hydrogen are going to fill the deep trapping sites of a metallic glass, resulting in a reduction of the barrier height and an *increase* of the diffusivity. At increased hydrogen concentration, a repulsive interaction between the hydrogen atoms will cause lattice expansion, so that the barrier will increase. In addition, site-blocking effect will become important, so that the diffusivity will *decrease*. An advanced discussion of this issue by means of the hydrogen density of states and the blocking effect may be found in a recent work of the Kirchheim's group [28]. One will, therefore, observe a bend-over of the diffusivity versus concentration at low H/M. This is indeed observed in Fig. 4b – the diffusion constant exhibits a weakly pronounced maximum at $H/M \approx 0.1$ and decreases significantly at higher concentrations. The almost constant values of E_a and D in the low H/M regime may, therefore, be interpreted to result from the overlap of three effects – while filling of the deep trapping sites decreases E_a and increases D, lattice expansion and site blocking act in the opposite way.

Regarding the decrease of D in the medium concentration range, $0.2 < H/M < 0.9$, the experimental precision of the data in Fig. 4b suggests a linear-like variation of D. In this concentration range, both effects – the increase of E_a due to lattice expansion and the decrease of D_0 due to site blocking – are expected to participate in the decrease of the diffusion constant. The observed linear-like variation of D resembles the prediction for the site-blocking effect, but the expected decrease of D from $H/M = 0.2$ to 0.9 (assuming the linear dependence of the prefactor $D_0 \propto 2 - x$) is $D_{0.2}/D_{0.9} = 1.6$, which is about two times smaller than the experimental value $D_{0.2}/D_{0.9} = 2.7$. On the other hand, the decrease of D due to the increase of E_a (from 402 meV at H/$M = 0.2$ to about 470 meV at $H/M = 0.9$) should be by a factor $D_{0.2}/D_{0.9} \approx 7$, which is a factor 2.6 larger than the experimental value (note that, due to

the exponential dependence of D on E_a, this estimate is uncertain as a small error in E_a causes large difference in the $D_{0.2}/D_{0.9}$ factor). The above $D_{0.2}/D_{0.9}$ values are of the same order of magnitude, so that it is not possible to assign the observed H/M dependence of D to a single mechanism in this intermediate hydrogen concentration range. We can anticipate that the decreased hydrogen diffusivity with increasing H/M is a consequence of both the E_a increase and the D_0 decrease.

In the high hydrogen concentration range, $H/M > 0.9$, neither D nor E_a change any more with further increase of the hydrogen concentration up to 1.9. For the icosahedral $Zr_{69.5}Cu_{12}Ni_{11}Al_{7.5}$, the concentration $H/M \approx 0.9$ was reported to be the one above which the sample transforms into a fully amorphous structure [11,24]. In addition, $H/M \approx 0.9$ is the concentration above which the ZrCuNiAl material becomes very brittle [29], indicating a mechanical failure of the amorphous ribbons. These results suggest that the H/M-independent D and E_a in the high-concentration range may not be intrinsic properties of the ZrCuNiAl BMG state, but occur due to hydrogenation-induced microstructural changes of the material. Such changes involve formation of crystalline hydride phases, which is supported by a strong decrease in the thermal stability of the glass at very high concentrations, $H/M > 0.9$, observed by differential scanning calorimetry (DSC) [30]; in addition, a nanocrystalline hydride phase was observed to form instead of tetragonal Zr_2Ni. The formation of a crystalline hydride phase at hydrogen contents above $H/M \approx 0.9$ is also known to result from hydrogenation from the gas phase at 250 °C [31]. As a result of microstructural changes, new diffusion paths are formed along the interfaces; these paths may not change with further increase in the hydrogen content, thus giving rise to the observed constant diffusivity above $H/M \approx 0.9$. Finally, one should not discard also the possible trivial contribution to the concentration-independent diffusion constant in the high H/M regime. Hydrogen may be stored in the microcracks and voids formed in the brittle material, providing parallel paths for the hydrogen diffusion extrinsic to the ZrCuNiAl BMG structure.

5. Conclusions

Hydrogen diffusion in the $Zr_{69.5}Cu_{12}Ni_{11}Al_{7.5}$ is two orders of magnitude slower as compared to simple-structure metal hydrides, but practically identical in the icosahedral and BMG states of this material, supporting the assumption that the same atomic SRO exists in both states. The determination of the H/M-dependence of D in the i-QC state was inconclusive due to small number of investigated samples, whereas the "high-resolution" study (in view of many samples hydrated to approximately evenly-spaced H/M values) of the BMG phase clearly showed the influence of the hydrogen content on its diffusivity. Within the investigated concentration range between 0 and 1.9, three regions can be defined. At low hydrogen concentration, $H/M < 0.2$, E_a and D exhibit weak concentration dependence, compatible with the model of Kirchheim that predicts a maximum in the diffusion constant at low H/M. In the intermediate regime, $0.2 < H/M < 0.9$, E_a increases significantly due to lattice expansion, whereas D_0 decreases due to site blocking, so that D decreases in a linear-like manner from $H/M = 0.2$ to 0.9 by a factor 2.7. In the high concentration range, $0.9 < H/M < 1.9$, D and E_a do not change any more with H/M. We propose that this H/M-independence results from opening of new paths for hydrogen diffusion that are extrinsic to the $Zr_{69.5}Cu_{12}Ni_{11}Al_{7.5}$ BMG state and originate in the hydrogenation-induced microstructural changes of the material. Finally, it is important to stress that the presented H/M-dependent study of the hydrogen diffusion in the $Zr_{69.5}Cu_{12}Ni_{11}Al_{7.5}$ material, performed by the SFF diffusion NMR experiment, shows high correlation between the hydrogen mobility in the lattice and the atomic-level structural changes of the material upon hydrogenation.

References

[1] See, for a, review: P.C. Gibbons, K.F. Kelton, in: Z.M. Stadnik (Ed.), Physical Properties of Quasicrystals. Springer Series in Solid-State Sciences, vol. 126, Springer, Berlin, 1999, p. 403.
[2] A.M. Viano, R.M. Stroud, P.C. Gibbons, A.F. McDowell, M.S. Conradi, K.F. Kelton, Phys. Rev. B 51 (1995) 12026.
[3] A. Shastri, E.H. Majzoub, F. Borsa, P.C. Gibbons, K.F. Kelton, Phys. Rev. B 57 (1998) 5148.
[4] K.R. Faust, D.W. Pfitsch, N.A. Stojanovich, A.F. McDowell, N.L. Adolphi, E.H. Majzoub, J.Y. Kim, P.C. Gibbons, K.F. Kelton, Phys. Rev. B 62 (2000) 11444.
[5] K. Foster, R.G. Leisure, J.B. Shaklee, J.Y. Kim, K.F. Kelton, Phys. Rev. B 61 (2000) 241.
[6] A.F. McDowell, N.L. Adolphi, C.A. Sholl, J. Phys.: Condens. Matter 13 (2001) 9799.
[7] U. Köster, J. Meinhardt, S. Roos, H. Liebertz, Appl. Phys. Lett. 69 (1996) 179.
[8] B.I. Wehner, J. Meinhardt, U. Köster, H. Alves, N. Eliaz, D. Eliezer, Mater. Sci. Eng. A 226–228 (1997) 1008.
[9] D. Zander, H. Leptien, U. Köster, N. Eliaz, D. Eliezer, J. Non-Cryst. Solids 250–252 (1999) 893.
[10] D. Zander, U. Köster, N. Eliaz, D. Eliezer, D. Plachke, in: J.M. Dubois, P.A. Thiel, A.P. Tsai, K. Urban (Eds.), Mater. Res. Soc. Symp. Proc., vol. 553, Materials Research Society, Warrendale, 1999, p. 49.
[11] D. Zander, U. Köster, V. Khare, in: E. Belin-Ferré, P.A Thiel, A.P. Tsai, K Urban (Eds.), Mater. Res. Soc. Symp. Proc., vol. 643, Materials Research Society, Warrendale, 2001, p. K2.2.1.
[12] T. Apih, V. Khare, M. Klanjšek, P. Jeglič, J. Dolinšek, Phys. Rev. B 68 (2003) 212202.
[13] T. Apih, M. Bobnar, J. Dolinšek, L. Jastrow, D. Zander, U. Köster, Solid State Commun. 134 (2005) 337.
[14] H. Smithson, C.A. Marianetti, D. Morgan, A. Van der Ven, A. Predith, G. Ceder, Phys. Rev. B 66 (2002) 144107.
[15] A.C. Switendick, Z. Phys. Chem. N. F. 117 (1979) 89.
[16] J. Völkl, G. Alefeld, in: A.S. Nowick, J.J. Burton (Eds.), Diffusion in Solids, Recent Developments, Academic, New York, 1975, p. 231.
[17] J. Völkl, G. Alefeld, in: G. Alefeld, J. Völkl (Eds.), Hydrogen in Metals. I. Basic Properties, Springer, Berlin, 1978, p. 321.
[18] R.C. Bowman Jr., in: G. Bambakidis (Ed.), Metal Hydrides, NATO ASI Series B, vol. 76, Plenum, New York, 1981, p. 109.
[19] E.O. Stejskal, J.E. Tanner, J. Chem. Phys. 42 (1965) 288.
[20] H. Züchner, H. Barlag, G. Majer, J. Alloys Compd. 330–332 (2002) 448.
[21] R. Kimmich, W. Unrath, G. Schnur, E. Rommel, J. Magn. Reson. 91 (1991) 136.
[22] I. Chang, F. Fujara, B. Geil, G. Hinze, H. Sillescu, A. Toelle, J. Non-Cryst. Solids 172–174 (1994) 674.
[23] P. Jeglič, A. Lebar, T. Apih, J. Dolinšek, J. Magn. Reson. 150 (2001) 39.
[24] D. Zander, U. Köster, in: H.-R. Trebin (Ed.), Quasicrystals, Structure and Physical Properties, Wiley–VCH, Weinheim, 2003, p. 629.
[25] C. Janot, J.-M. Dubois, in: J.-B. Suck, M. Schreiber, P. Häussler (Eds.), Quasicrystals, An Introduction to Structure, Physical Properties and

Applications, Springer Series in Materials Science, vol. 55, Springer, Berlin, 2002, p. 183.
[26] A.S. Bakai, in: H. Beck, H.-J. Güntherodt (Eds.), Glassy Metals. III. Topics in Applied Physics, vol. 72, Springer, Berlin, 1994, p. 209.
[27] U. Stolz, U. Nagorny, R. Kirchheim, Scripta Metall. 18 (1984) 347.
[28] J. Bankmann, Löslichkeit und Diffusion von Wasserstoff in dünnen Schichten amorpher ZrTiNiCuBe- und ZrAlNiCi-Legierungen, Ph.D. Thesis, University of Göttingen, 2002.
[29] U. Köster, D. Zander, J. Meinhardt, N. Eliaz, D. Eliezer, in: S. Takeuchi, T. Fujiwara (Eds.), Proceedings of the Sixth International Conference on Quasicrystals, Tokyo, 1996, World Scientific, Singapore, 1997 , p. 313.
[30] D. Zander, Wasserstoff in metastabilen Zr–Cu–Ni–Al Legierungen, Ph.D. Thesis, University of Dortmund, Logos Verlag, Berlin, 2001.
[31] V.T. Huett, D. Zander, L. Jastrow, E.H. Majzoub, K.F. Kelton, U. Köster, J. Alloys Compd. 379 (2004) 16.